Tetrahedrality Dictates Dynamics in Hard Sphere Mixtures

Susana Marín-Aguilar, Henricus H. Wensink, Giuseppe Foffi,* and Frank Smallenburg†
Université Paris-Saclay, CNRS, Laboratoire de Physique des Solides, 91405 Orsay, France

(Received 9 December 2019; accepted 1 May 2020; published 22 May 2020)

The link between local structure and dynamical slowdown in glassy fluids has been the focus of intense debate for the better part of a century. Nonetheless, a simple method to predict the dynamical behavior of a fluid purely from its local structural features is still missing. Here, we demonstrate that the diffusivity of perhaps the most fundamental family of glass formers—hard sphere mixtures—can be accurately predicted based on just the packing fraction and a simple order parameter measuring the tetrahedrality of the local structure. Essentially, we show that the number of tetrahedral clusters in a hard sphere mixture is directly linked to its global diffusivity. Moreover, the same order parameter is capable of locally pinpointing particles in the system with high and low mobility. We attribute the power of the local tetrahedrality for predicting local and global dynamics to the high stability of tetrahedral clusters, the most fundamental building and densest-packing building blocks for a disordered fluid.

DOI: 10.1103/PhysRevLett.124.208005

Hard spheres are arguably the most fundamental model system in colloidal science, for theory, simulation, and experiment alike. Over many decades of study, hard spheres have been instrumental in cementing our understanding of the physics of, e.g., entropy-driven phase transitions, crystal nucleation, and the glass transition [1–8]. Hard particles, despite their simplicity, serve as a basic approach to model the rheology of dense suspensions [9] with applications in cell biology [10], food science [11], and geology [12]. Although monodisperse systems of hard spheres readily crystallize into simple close-packed crystals, mixtures of hard spheres of different sizes can form a zoo of exotic structures [13,14], and are hence a promising route to the creation of new materials with well-controlled structure on the microscopic scale. Additionally, hard sphere mixtures are also prototypical glass formers [15,16], and close to the regime where crystallization is expected, their dynamics often slow down dramatically [17]. As a result, understanding the dynamics of hard sphere mixtures close to the glass transition is a vital ingredient for optimal control over their crystallization behavior.

One of the interesting features of glassy hard sphere mixtures is the fact that their dynamics can be tuned not only via packing fraction, but also by varying the size and number ratios of the different species [18–20]. Intuitively, mixing spheres of different sizes results in different geometrical constraints on the possible local packings of particles, and hence this will lead to different local structures. This will inevitably also impact dynamics, although the exact nature of the link between structure and dynamics in glassy materials remains a topic under heavy debate [21–26]. A number of studies have linked dynamical slowdown to the emergence of local structural patterns, that are favored by entropy and/or energy and hence likely to survive for a long time (see, e.g., Refs. [27–33]). This idea of locally favored structures originates from the seminal work of Frank [34], who conjectured that glasses may result from the formation of icosahedral clusters, which are not capable of globally filling space regularly. More recently, many studies have focused on quantifying local structure in a variety of ways, with the aim of finding good predictors for the dynamics of different glass formers. For comprehensive comparisons of many of these methods, we suggest, e.g., the recent reviews in Refs. [23,24]. In general, the emerging picture is that, for many glass formers, we can identify long-lived structures whose presence is strongly correlated with the global slowdown of dynamics in glasses. However, our ability to predict the mobility of *individual* particles based on local structure depends strongly on the system under consideration [35,36].

In this Letter, we examine the link between local structure and dynamics in simulations of hard sphere mixtures. We quantify local order via the tetrahedrality of the local structure (TLS), a simple idea which consists of counting the number of tetrahedral clusters around each particle. As they consist of only 4 particles linked together, they can be considered as the smallest locally favored structures. Various order parameters based on local (poly) tetrahedral order have previously been shown to correlate with glassy dynamics in soft spheres [37], granular systems [38], and hard spheres [39,40]. Our results show that TLS not only has an impressively strong correlation with local dynamics, but is also able to quantitatively predict the diffusivity of a vast range of dense hard sphere mixtures. As perfect icosahedra can be broken down into tetrahedra, TLS is a natural extension of Frank's idea, but focuses on the most elementary building block of the three-dimensional fluid. Hence, we argue that tetrahedra are

the slow structures that are ultimately responsible for dynamic arrest.

We study the structure and dynamics of various mixtures of hard spheres of different sizes, using event-driven molecular dynamics simulations [41] at constant number of particles N, volume V, and energy E. All particles have identical mass m. The time unit of the simulation is given by $\tau = \sqrt{\beta m \sigma^2}$, with σ the diameter of the large spheres (for binary mixtures), or the average sphere size (for polydisperse mixtures), and $\beta = 1/k_B T$, with k_B Boltzmann's constant and T the temperature. All systems contained at least $N = 700$ particles, with more particles used ($N \gtrsim 2000$) for the slower systems.

We begin our study by exploring the structure and dynamics of dense binary hard sphere mixtures, varying the size ratio $q = \sigma_S/\sigma_L$ (with $\sigma_{S(L)}$ the diameter of the small (large) spheres), and the composition x_L, which denotes the fraction of large spheres. For each choice of q and x_L, we prepare the system at a packing fraction of $\eta = 0.575$, allow it to equilibrate, and measure the diffusion time $\tau_D = \sigma_L^2/D$, with D the diffusion coefficient. Note that we only consider systems which avoid crystallization; as a result, we cannot probe compositions close to 0 or 1, or size ratios close to $q = 1$, which all result into crystallization into a fcc crystal of (mostly) large spheres. Additionally, in our larger systems ($N \geq 2000$), we observe crystallization into Laves phases crystals for size ratio $q = 0.8$ [17,42], compositions close to $1/3$, and high packing fractions ($\eta \gtrsim 0.57$). These crystals are detected using a machine-learning-based order parameter [43].

The dynamics of binary hard sphere mixtures are known to vary significantly upon changing the composition x_L and size ratio q [18,19]. Our systematic investigation confirms this observation, as shown in Fig. 1(a), where we plot the diffusion time τ_D as a function of x_L for different size ratios q. Intriguingly, even though the packing fractions of all systems are the same, τ_D varies by more than an order of magnitude. Moreover, the dependence of τ_D on x_L is nonmonotonic, and shows qualitatively different behavior for different size ratios. For mixtures with a small size ratio $q \lesssim 0.75$, the diffusion time is a convex function of x_L, showing a clear single minimum. In contrast, for higher size ratios, a maximum in the diffusion times appears, corresponding to some of the slowest systems we investigated.

The composition and size ratio of a hard sphere mixture control the geometry of local packings in the fluid. Hence, the strong variation in diffusivity in Fig. 1(a) hints at strong variations in the local structure of these different systems as well. As local icosahedral order is known to slow down dynamics [23,34,35,44], we measure the fraction of particles involved in at least one local icosahedral cluster [as determined via the topological cluster classification algorithm [45,46]]. As shown in Fig. 1(b), the fraction of particles in an icosahedral environment indeed shows behavior similar to that of the diffusion time. However,

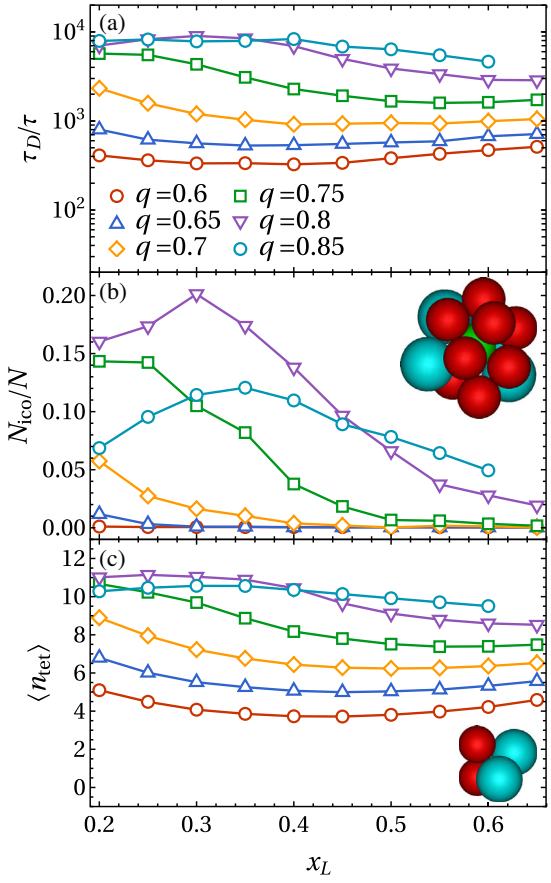

FIG. 1. (a) Diffusion time τ_D as a function of composition x_L for binary hard sphere mixtures with various size ratios q as indicated. τ is the time unit of the simulation. (b) Fraction of particles inside an icosahedral cluster for the same systems. The inset shows a typical icosahedral cluster. (c) Average number of tetrahedra per particle. The inset shows a typical tetrahedral cluster.

Fig. 1(b) clearly does not reproduce all of the behavior of the diffusion time in Fig. 1(a), and hence it is unlikely that icosahedra can be seen as the only slow structural motif in the system. Indeed, recent work has shown that a variety of complex clusters in hard sphere mixtures can have long lifetimes [31], and searching for these motifs in our systems reveals a whole family of clusters that commonly appear together with perfect icosahedral clusters [see Supplemental Material (SM) [47]]. Intuitively, it is therefore likely that each of these contributes, to some degree, to the slowdown of the system.

Interestingly, one feature shared by all of these local structural motifs is their incorporation of a large number of smaller tetrahedral clusters: groups of four particles in which each pair are considered nearest neighbors (here defined via the same modified Voronoi construction as used in the topological cluster classification algorithm [45]). Hence, a natural question to ask is whether the overall tetrahedrality of the local structure can predict dynamical behavior. As essentially all particles are involved in

multiple tetrahedral clusters, we quantify tetrahedrality by measuring the average number n_{tet} of tetrahedra a particle is involved in, and plot the results in Fig. 1(c) for each binary mixture. As an example, the central particle in the icosahedral cluster in Fig. 1(b) is part of 20 tetrahedra. This simple structural order parameter captures the behavior of the diffusion time almost perfectly, reproducing both the convexity of τ_D for low q and its maximum at high q. Similar agreement is observed at other packing fractions (see SM [47]). Note that TLS is based on counting the number of tetrahedra per particle and is fundamentally different from the parameter introduced in Ref. [37], which measures the local packing efficiency based on tetrahedral subvolumes.

The strong correlation between tetrahedrality and diffusivity becomes even clearer when we plot the relationship between these two quantities directly. In Fig. 2, we plot τ_D versus $\langle n_{\mathrm{tet}}\rangle$ for all investigated size ratios and compositions, and for a range of packing fractions. For each packing fraction, n_{tet} provides an excellent predictor of the diffusion time, revealing an approximately exponential relationship between τ_D and $\langle n_{\mathrm{tet}}\rangle$ (dashed lines). Note that just the set of blue triangles in Fig. 2 covers *all* 60 different systems in Fig. 1, with vastly different size ratios and compositions. Moreover, this data collapse is not restricted to binary systems: polydisperse systems fall on the same lines for all investigated polydispersities, ranging from 1% to 20% (closed symbols in Fig. 2). This strongly suggests that this behavior is universal for all mixtures of hard spheres of roughly similar sizes. Note that for more extreme size ratios than the ones studied here, demixing could occur due to stronger depletion effects [49].

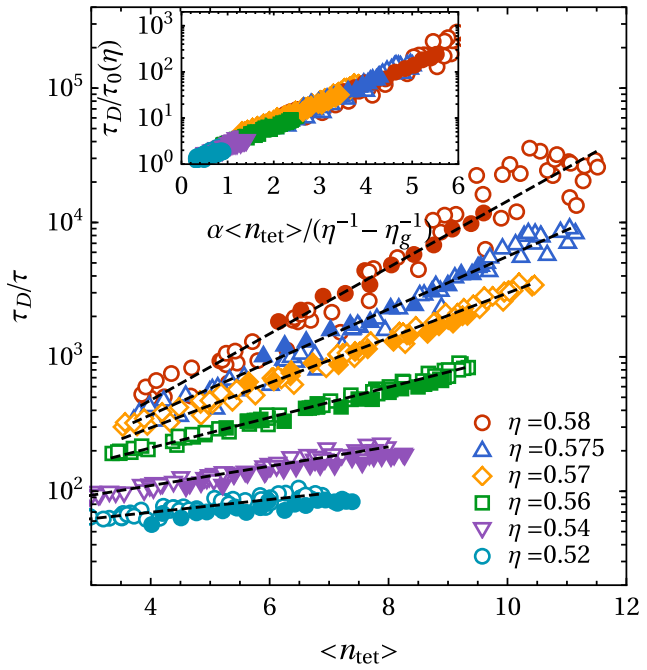

FIG. 2. Diffusion time for all investigated hard sphere mixtures as a function of tetrahedrality. Different colors indicate different packing fractions. Within each packing fraction, open symbols correspond to binary mixtures with different size ratios and compositions. Closed symbols are polydisperse systems with different packing fractions. The dashed lines are exponential fits to the binary data for each packing fraction. The inset shows the approximate data collapse obtained by rescaling the data according to Eq. (1).

Interestingly, we can approximately collapse the data for all packing fractions in Fig. 2 by assuming the diffusion time follows a Vogel-Fulcher-Tamman-like [50] relation,

$$\tau_D = \tau_0(\eta)\exp\left(\frac{\alpha\langle n_{\mathrm{tet}}\rangle}{\eta^{-1}-\eta_g^{-1}}\right), \tag{1}$$

where $\tau_0(\eta)$, $\alpha \simeq 0.03$, and $\eta_g \simeq 0.598$ are fit parameters, with only τ_0 dependent on the packing fraction. For the structural relaxation time τ_α, this relation does not apply as a consequence of the well-known violation of the Stokes-Einstein relation that occurs in glassy systems [21,28,51,52] (see SM [47]). As the inset of Fig. 2 shows, rescaling the data according to this fit indeed results in an approximate data collapse. However, the assumption of one universal value for η_g, for all combinations of size ratio and composition is likely not physical, as it is unlikely that the diffusion time diverges at the same packing fraction η_g for all mixtures. Indeed, additional simulations show that we can equilibrate some of our (less tetrahedral) systems at packing fractions close to and even beyond η_g (see SM [47]), and hence Eq. (1) must break down for sufficiently high η. Nonetheless, the data collapse indicates that Eq. (1) approximately captures the increased sensitivity of the dynamics to tetrahedrality as the packing fraction increases.

Thus far we have examined the relationship between globally averaged TLS and diffusivity. We now turn our attention to the impact of tetrahedral clusters on dynamics at a local level. To this end, we explore the relationship between the number of tetrahedra $n_{\mathrm{tet}}(i)$ a given particle i is involved in and the absolute distance δr_i over which it moves in a given time interval δt. In Figs. 3(a) and 3(b), we show a typical snapshot of one of our slowest noncrystallizing systems, with particles colored by either their tetrahedrality [Fig. 3(a)] or their displacement after a time interval $\delta t = 200\tau$ in a typical trajectory [Fig. 3(b)]. There is clear evidence of correlation between the two quantities, with regions of low tetrahedrality matching regions of high mobility (red), and vice versa (blue). However, examining the displacement in a specific trajectory provides only a limited view of particle mobility. After all, in a given trajectory, the ability of a particle to move depends not only on its environment but also on the initial velocities of all particles. To average out this thermal noise, we measure the dynamic propensity D_i of a particle: its average absolute displacement, taken over an ensemble of simulations starting from the same initial configuration [35,37,53]. In Fig. 3(c),

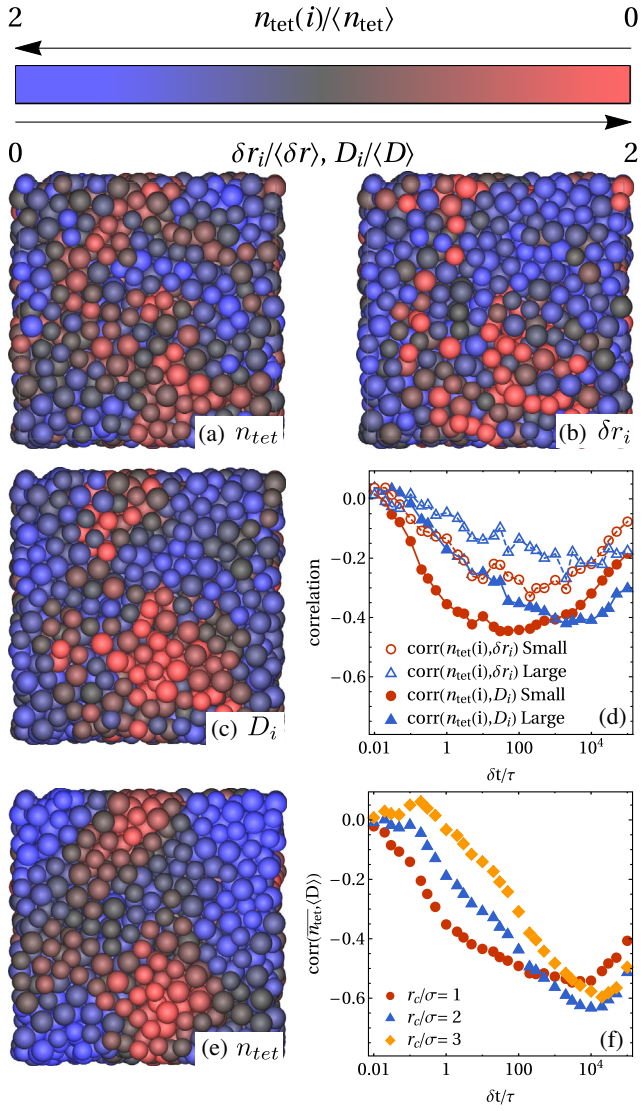

FIG. 3. (a–(c) Snapshot of a glassy system at packing fraction $\eta = 0.58$, size ratio $q = 0.85$, and composition $x_L = 0.3$, with particles colored according to different criteria: (a) according to the number of tetrahedra $n_{\text{tet}}(i)$ a particle is involved in, with red particles involved in fewer tetrahedra, and blue particles in more, (b) according to the absolute displacement δr_i after a time interval $\delta t = 200\tau$ in one trajectory, with red indicating fast particles and blue indicating slow ones, (c) according to the dynamic propensity D_i over the same δt. In all snapshots, pure gray indicates the average for both large and small particles. (d) Spearman's rank correlation between the number of tetrahedral clusters a particle is involved in n_{tet} and either its displacement δr_i (open symbols) or its dynamic propensity D_i (closed symbols), measured over a time interval δt. (e) Same snapshot, but colored by average tetrahedrality over a spherical region of radius $r_c = 2\sigma$ around each particle. (f) Correlation between locally averaged tetrahedrality and D_i for different radii r_c of the averaging region.

we color each particle according to D_i (again taken at $\delta t = 200\tau$), and indeed reveal a striking correlation between n_{tet} and D_i. Clearly, local tetrahedrality is an excellent predictor for the dynamics of a particle in the near future.

This correlation can be quantified explicitly by calculating the Spearman's rank-order correlation between $n_{\text{tet}}(i)$ and D_i. In Fig. 3(d), we plot this correlation as a function of the time interval δt for both the small and large particles. At very short timescales ($\delta t \lesssim 0.1\tau$), before any particles escape their cages, there is little correlation between local TLS and dynamic propensity. At intermediate timescales, we find a strong negative correlation between $n_{\text{tet}}(i)$ and D_i, confirming that particles involved in fewer tetrahedra are more mobile. Finally, for timescales approaching the diffusion time $\tau_D \approx 10^4\tau$, the memory of the initial configuration is lost, the initial tetrahedral clusters are broken up (see SM [47]) [54], and the correlations start decaying back to zero. An examination of these correlations in other hard sphere mixtures provides similar results, with weaker correlations for systems with higher diffusivity (see SM [47]). In faster systems, dynamics are less heterogeneous, and hence less predictable based on local structure.

The level of correlation between TLS and dynamic propensity demonstrated outperforms most of the purely local observables previously investigated [24]. Moreover, as shown previously for other local order parameters [24,35], the predictive power of TLS can be enhanced by performing a local averaging of n_{tet}. To this end, we define $\overline{n_{\text{tet}}}(i, r_c)$ as the mean value of $n_{\text{tet}}(j)$ for all particles j found within a sphere of radius r_c around particle i (including i itself). This is illustrated in Fig. 3(e), in which we have colored particles by their value of $\overline{n_{\text{tet}}}(i, r_c = 2\sigma)$. As one might expect, this results in smoother domains of high tetrahedrality, which correlate yet more strongly with the dynamical propensity shown in Fig. 3(c). The corresponding Spearman's correlation coefficients for the small particles are plotted in Fig. 3(f) for three different cutoff radii r_c. This correlation is optimized for $r_c = 2\sigma$, at a value of ≈ 0.63. In Ref. [35], similarly strong correlations between dynamical propensity and (larger) locally preferred structures were found for the Wahnström model glass former [55], but not for several other model glass formers, such as the Kob-Andersen mixture [56]. Using TLS, we find similar results for these models (see SM [47]).

The results in this Letter paint an elegant and comprehensive picture of the relationship between local structure and dynamics in hard sphere mixtures. On the local level, examining tetrahedrality reveals large-scale regions of particles involved in a large number of tetrahedra, corresponding directly to areas of low mobility. Globally, the tetrahedrality directly predicts diffusivity at each investigated packing fraction, resulting in a data collapse of a vast variety of hard sphere mixtures onto one exponential curve using only two global fit parameters. This demonstrates that within this family of hard sphere mixtures, tetrahedra play a predictable and universal role in determining dynamics. In comparison, a similar data collapse in recent work on a (more varied) set of systems [25] required

multiple fit parameters per system, limiting its predictive power.

These predictions can be directly tested in experimental realizations of colloidal hard sphere mixtures, using, e.g., confocal microscopy [57–62]. Our results may impact attempts to realize the self-assembly of binary Laves phases [17,63], for which the stability region is in the regime where dynamics are extremely slow. On the theoretical side, the exponential dependence of global dynamics on tetrahedrality is strongly reminiscent of theoretical descriptions of glasses in terms of activation energies for collective rearrangement [64] and random first-order transition theory [21,65,66]. Most importantly, our results demonstrate that the dynamics of hard sphere mixtures can be predicted purely by looking for the most fundamental three-dimensional building block for the fluid: the simple tetrahedron.

We thank Francesco Sciortino and Laura Filion for useful discussions, and Saheli Mitra for her help with the Wahnström and Kob-Andersen simulations. S. M.-A. acknowledges CONACyT for funding (scholarship 340015/471710).

*giuseppe.foffi@u-psud.fr
†frank.smallenburg@u-psud.fr

[1] P. N. Pusey and W. van Megen, Phys. Rev. Lett. **59**, 2083 (1987).
[2] W. van Megen and S. M. Underwood, Phys. Rev. Lett. **70**, 2766 (1993).
[3] E. R. Weeks, J. C. Crocker, A. C. Levitt, A. Schofield, and D. A. Weitz, Science **287**, 627 (2000).
[4] L. Berthier, G. Biroli, J.-P. Bouchaud, L. Cipelletti, D. El Masri, D. L'Hôte, F. Ladieu, and M. Pierno, Science **310**, 1797 (2005).
[5] G. Brambilla, D. El Masri, M. Pierno, L. Berthier, L. Cipelletti, G. Petekidis, and A. B. Schofield, Phys. Rev. Lett. **102**, 085703 (2009).
[6] W. K. Kegel and A. van Blaaderen, Science **287**, 290 (2000).
[7] G. Parisi and F. Zamponi, Rev. Mod. Phys. **82**, 789 (2010).
[8] J. Barrat, W. Gotze, and A. Latz, J. Phys. Condens. Matter **1**, 7163 (1989).
[9] J. J. Stickel and R. L. Powell, Annu. Rev. Fluid Mech. **37**, 129 (2005).
[10] E. H. Zhou, X. Trepat, C. Y. Park, G. Lenormand, M. N. Oliver, S. M. Mijailovich, C. Hardin, D. A. Weitz, J. P. Butler, and J. J. Fredberg, Proc. Natl. Acad. Sci. U.S.A. **106**, 10632 (2009).
[11] C. Servais, R. Jones, and I. Roberts, J. Food Eng. **51**, 201 (2002).
[12] S. M. Wickham, J. Geol. Soc. **144**, 281 (1987).
[13] P. K. Bommineni, N. R. Varela-Rosales, M. Klement, and M. Engel, Phys. Rev. Lett. **122**, 128005 (2019).
[14] L. Filion and M. Dijkstra, Phys. Rev. E **79**, 046714 (2009).
[15] P. Pusey, E. Zaccarelli, C. Valeriani, E. Sanz, W. C. Poon, and M. E. Cates, Phil. Trans. R. Soc. A **367**, 4993 (2009).
[16] E. Sanz, C. Valeriani, E. Zaccarelli, W. C. Poon, M. E. Cates, and P. N. Pusey, Proc. Natl. Acad. Sci. U.S.A. **111**, 75 (2014).
[17] T. Dasgupta, G. M. Coli, and M. Dijkstra, arXiv:1906.10680.
[18] W. Götze and T. Voigtmann, Phys. Rev. E **67**, 021502 (2003).
[19] G. Foffi, W. Götze, F. Sciortino, P. Tartaglia, and T. Voigtmann, Phys. Rev. Lett. **91**, 085701 (2003).
[20] E. Lázaro-Lázaro, J. A. Perera-Burgos, P. Laermann, T. Sentjabrskaja, G. Pérez-Ángel, M. Laurati, S. U. Egelhaaf, M. Medina-Noyola, T. Voigtmann, R. Castañeda-Priego, and L. F. Elizondo-Aguilera, Phys. Rev. E **99**, 042603 (2019).
[21] L. Berthier and G. Biroli, Rev. Mod. Phys. **83**, 587 (2011).
[22] F. H. Stillinger and P. G. Debenedetti, Annu. Rev. Condens. Matter Phys. **4**, 263 (2013).
[23] C. P. Royall and S. R. Williams, Phys. Rep. **560**, 1 (2015).
[24] H. Tanaka, H. Tong, R. Shi, and J. Russo, Nat. Rev. Phys. **1**, 333 (2019).
[25] H. Tong and H. Tanaka, Nat. Commun. **10**, 5596 (2019).
[26] R. Pastore, A. Coniglio, A. de Candia, A. Fierro, and M. P. Ciamarra, J. Stat. Mech. (2016) 054050.
[27] D. Coslovich and G. Pastore, J. Chem. Phys. **127**, 124504 (2007).
[28] M. Dzugutov, S. I. Simdyankin, and F. H. M. Zetterling, Phys. Rev. Lett. **89**, 195701 (2002).
[29] J. P. K. Doye, D. J. Wales, F. H. M. Zetterling, and M. Dzugutov, J. Chem. Phys. **118**, 2792 (2003).
[30] G. Tarjus, S. A. Kivelson, Z. Nussinov, and P. Viot, J. Phys. Condens. Matter **17**, R1143 (2005).
[31] C. P. Royall, A. Malins, A. J. Dunleavy, and R. Pinney, J. Non-Cryst. Solids **407**, 34 (2015).
[32] M. Campo and T. Speck, J. Chem. Phys. **152**, 014501 (2020).
[33] J. E. Hallett, F. Turci, and C. P. Royall, Nat. Commun. **9**, 3272 (2018).
[34] F. C. Frank, Proc. R. Soc. A **215**, 43 (1952).
[35] G. M. Hocky, D. Coslovich, A. Ikeda, and D. R. Reichman, Phys. Rev. Lett. **113**, 157801 (2014).
[36] R. L. Jack, A. J. Dunleavy, and C. P. Royall, Phys. Rev. Lett. **113**, 095703 (2014).
[37] H. Tong and H. Tanaka, Phys. Rev. X **8**, 011041 (2018).
[38] C. Xia, J. Li, Y. Cao, B. Kou, X. Xiao, K. Fezzaa, T. Xiao, and Y. Wang, Nat. Commun. **6**, 8409 (2015).
[39] A. V. Anikeenko and N. N. Medvedev, Phys. Rev. Lett. **98**, 235504 (2007).
[40] B. Charbonneau, P. Charbonneau, and G. Tarjus, Phys. Rev. Lett. **108**, 035701 (2012).
[41] D. C. Rapaport, *The Art of Molecular Dynamics Simulation* (Cambridge University Press, Cambridge, UK, 2004).
[42] A.-P. Hynninen, L. Filion, and M. Dijkstra, J. Chem. Phys. **131**, 064902 (2009).
[43] E. Boattini, M. Ram, F. Smallenburg, and L. Filion, Mol. Phys. **116**, 3066 (2018).
[44] S. Marín-Aguilar, H. H. Wensink, G. Foffi, and F. Smallenburg, Soft Matter **15**, 9886 (2019).
[45] A. Malins, S. R. Williams, J. Eggers, and C. P. Royall, J. Chem. Phys. **139**, 234506 (2013).

[46] A. Malins, J. Eggers, C. P. Royall, S. R. Williams, and H. Tanaka, J. Chem. Phys. **138**, 12A535 (2013).
[47] See Supplemental Material at http://link.aps.org/supplemental/10.1103/PhysRevLett.124.208005 for additional data and simulation details, which includes Ref. [48].
[48] S. Plimpton, Fast parallel algorithms for short-range molecular dynamics, Technical Report, Sandia National Labs, 1993, http://lammps.sandia.gov.
[49] V. J. Anderson and H. N. Lekkerkerker, Nature (London) **416**, 811 (2002).
[50] L. S. García-Colín, L. F. del Castillo, and P. Goldstein, Phys. Rev. B **40**, 7040 (1989).
[51] S. Sengupta, S. Karmakar, C. Dasgupta, and S. Sastry, J. Chem. Phys. **138**, 12A548 (2013).
[52] S. Wei, Z. Evenson, M. Stolpe, P. Lucas, and C. A. Angell, Sci. Adv. **4**, eaat8632 (2018).
[53] A. Widmer-Cooper, P. Harrowell, and H. Fynewever, Phys. Rev. Lett. **93**, 135701 (2004).
[54] As shown in the SM, the autocorrelation function corresponding to the evolution of n_{tet} for a given particle decays over a timescale that is significantly shorter than τ_D [47]. This is to be expected, as the particle displacements that are required for local rearrangements which change the number of tetrahedral clusters around a particle are significantly smaller than σ_L.
[55] G. Wahnström, Phys. Rev. A **44**, 3752 (1991).
[56] W. Kob and H. C. Andersen, Phys. Rev. E **51**, 4626 (1995).
[57] E. Martinez-Sotelo, M. Escobedo-Sánchez, and M. Laurati, J. Chem. Phys. **151**, 164504 (2019).
[58] M. Laurati, P. Maßhoff, K. J. Mutch, S. U. Egelhaaf, and A. Zaccone, Phys. Rev. Lett. **118**, 018002 (2017).
[59] J. Baumgartl, R. P. A. Dullens, M. Dijkstra, R. Roth, and C. Bechinger, Phys. Rev. Lett. **98**, 198303 (2007).
[60] J. M. Lynch, G. C. Cianci, and E. R. Weeks, Phys. Rev. E **78**, 031410 (2008).
[61] T. Narumi, S. V. Franklin, K. W. Desmond, M. Tokuyama, and E. R. Weeks, Soft Matter **7**, 1472 (2011).
[62] S. Vivek, C. P. Kelleher, P. M. Chaikin, and E. R. Weeks, Proc. Natl. Acad. Sci. U.S.A. **114**, 1850 (2017).
[63] D. Wang, T. Dasgupta, E. B. van der Wee, D. Zanaga, T. Altantzis, Y. Wu, G. M. Coli, C. B. Murray, S. Bals, M. Dijkstra, and A. van Blaaderen, arXiv:1906.10088.
[64] G. Adam and J. H. Gibbs, J. Chem. Phys. **43**, 139 (1965).
[65] T. R. Kirkpatrick, D. Thirumalai, and P. G. Wolynes, Phys. Rev. A **40**, 1045 (1989).
[66] J.-P. Bouchaud and G. Biroli, J. Chem. Phys. **121**, 7347 (2004).